NASA TECHNICAL MEMORANDUM

NASA TM X-71439

NASA TM X-71439

COMPARISON OF GROUND AND FLIGHT TEST RESULTS USING A MODIFIED F106B AIRCRAFT

by Fred A. Wilcox
Lewis Research Center
Cleveland, Ohio, 44135

TECHNICAL PAPER proposed for presentation at Ninth Propulsion Joint Specialist Conference cosponsored by the American Institute of Aeronautics and Astronautics and the Society of Automotive Engineers
Las Vegas, Nevada, November 5-7, 1973

COMPARISON OF GROUND AND FLIGHT TEST RESULTS USING A MODIFIED F106B AIRCRAFT

Fred A. Wilcox
Lewis Research Center
National Aeronautics and Space Administration
Cleveland, Ohio 44135

E-7695

Abstract

Two aft underwing nacelles housing afterburning J85 engines were added to an F106 to study exhaust nozzles in flight at Mach numbers up to 1.3. Installation effects were determined for several nozzles by comparing flight data to data from an isolated wind tunnel model. Reynolds number effects were studied at subsonic flight speeds for nozzles intended for use with afterburning turbofan engines. A wide range of Reynolds number was obtained by flying the F106 over a range of altitude and by using 5 and 22% wind tunnel models of the F106. A contoured nozzle had a boattail drag as low as that of a longer circular arc nozzle over the Reynolds number range studied.

Take-off flight velocity (M_0 = 0.4) effects on noise suppression and thrust of supersonic cruise type nozzles and several noise suppression nozzles were studied by comparing flyover data with static data. Peak noise levels measured in flyover were generally higher than predicted from static data. Thrust performance of noise suppression nozzles was degraded in flyover. When data were scaled to full size engines and a sideline distance of 2128 ft noise suppression effectiveness of 14.5 EPNdb was obtained with 14.3% loss in thrust.

Introduction

A flight test program was undertaken by the Lewis Research Center using a modified F106B. Modifications to the aircraft were made at the Lewis Research Center and flight tests were begun in 1968. The purpose of the original program was to study installation effects at transonic speeds for propulsion systems applicable to supersonic transport aircraft. Performance data could be obtained from propulsion system components such as complex exhaust nozzles that could not be tested in wind tunnels because of transonic model size limitations.

The F106 was modified to incorporate two 25 inch diameter underwing nacelles housing afterburning J85 engines. Provisions were made to mount various exhaust nozzles behind them and measure their overall thrust minus drag and component drags. Many exhaust nozzles of various types were subsequently built and flight tested. More than 240 flights have been made to date.

The original objectives of the flight program have since been expanded to include other areas. One of these was the study of the effect of Reynolds number on nozzle boattail drag. Another was the study of flight effects on jet noise. In addition, flight tests on inlets are now being conducted. In carrying out these objectives, tests were also conducted in the Lewis 8- by 6-foot supersonic tunnel with scale models and on the F106 to statically measure jet noise. The purpose of this paper is to discuss results that were obtained in the above mentioned areas of exhaust nozzle technology where the unique capabilities of the flight program contributed to understanding.

Apparatus and Procedure

Modifications to Aircraft

The modifications to the aircraft (Fig. 1) are described in References 1 to 5 and will be briefly summarized herein. The two research nacelles added to the aircraft were located symmetrically at the 32% semi-span position. The nacelles were attached to the wing by means of two bearing supported links. Load cells to measure thrust minus drag were connected between the nacelles and the wing. Fuel for the J85 engines was separate from the main aircraft system and was contained in a tank located in the missile bay. A digital and an analog data system were located onboard. The digital data system described in Reference 4 used 10 scani valves which provided the capability of measuring 480 pressures along with 96 other parameters. Data were obtained at flight Mach numbers from 0.4 to 1.3 and at altitudes from sea level to 55,000 ft.

Wind Tunnel Models

The models that were used in the 8×6 tunnel to complement the flight program are shown in Figure 2. To determine installation effects, nozzles were initially tested on an $8\frac{1}{2}$ inch diameter isolated cold jet model. A wide variety of nozzles were studied on this model at external flow Mach numbers up to 2.0.(6-19) This isolated performance data was then compared to installed data obtained from flight and from scaled wind tunnel F106 models.

The 5% scale F106 model was used to study alternate nacelle configurations and the less complex nozzles. This model incorporated jet boundary simulators and nozzle performance was determined by integrating boattail pressures. Results from this model are reported in References 20 to 23. Reference 24 is a flow survey under the wing with no nacelles attached.

The 22% half-span F106 model was mounted on a reflection plate and incorporated a powered turbojet engine simulator. A description of the simulator and its operation is given in Reference 25.

Description of Nozzles

Some of the exhaust nozzles used in the program are shown in Figure 3. More complete descriptions of these nozzles and their flight performance data are given in References 26-31. Four supersonic cruise nozzles are shown in Figure 3(a). They all had, in concept, variable features which allowed them to cruise efficiently at both supersonic and subsonic flight speeds. They are all shown in the subsonic cruise configuration. The variable flap ejector (VFE) was fixed but in concept had trailing edge flaps that formed the boattail surface. At subsonic cruise this nozzle had

the largest boattail projected area of all these nozzles and a 15° boattail angle. The auxiliary inlet ejector (AIE) had inlets to admit external air at low values of nozzle pressure ratio. This reduced the required amount of boattailing.

The plug nozzle, in concept, had a fixed conical centerbody and a translating outer shroud which would extend to provide the required area ratio at high nozzle pressure ratio. The version shown was uncooled and was operated with the J85 engine in a nonafterburning mode. A convection cooled version of this nozzle was also built and flight tested on the F106 with the J85 engine operating to maximum afterburning.(32) Cooling air was bled from the J85 compressor.

The wedge nozzle also had a shroud which, in concept, could be translated. This nozzle type has potential advantages for twin pod installations where the wedge can fill in the interfairing region. The internal performance of this nozzle is reported in Ref. 33. The triangular sideplates shown in the photograph were removed for the installation effect data at Mach number 0.9 in order to obtain a comparison with isolated data from Ref. 33. Noise data were taken with sideplates installed. The wedge was mounted horizontally as shown for flight tests. It was rotated to a vertical position for static noise measurements.

The nozzles shown in Fig. 3(b) are suitable for use on military aircraft having supersonic dash capability and powered by afterburning turbofan engines. Three different approaches to boattail design are represented. These nozzles were of the variable flap type but had much larger boattail projected area and steeper boattail angles than the supersonic cruise nozzles of Fig. 3(a). The circular arc-conic nozzle had a 0.65 radius ratio arc which blended into a 24° cone.(34,35) Radius ratio is defined as the ratio of the radius of the boattail shoulder to the radius of a complete circular arc nozzle, with the same boattail angle and ratio of nozzle exit area to nacelle area. The circular arc nozzle was a complete circular arc having a 24° angle at the trailing edge (radius ratio 1.00 nozzle of Ref. 34). The contoured nozzle had a boattail with a very gradual initial turn given by the coordinates on Fig. 3(c) with boattail angles as high as 31°.

Some of the noise suppression nozzles tested are shown on Fig. 3(d). The philosophy behind these nozzles was to divide the main jet into small jets and provide mixing with external air to lower the jet velocity and thus reduce noise. A greater portion of the noise energy will also be at higher frequencies where the atmosphere is effective in providing attenuation at large sideline distances. More complete descriptions of these nozzles and performance results are given in Refs. 36 to 41.

The nozzle geometry to accomplish these objectives is generally not suitable for use at cruise conditions and thus has to be made retractable. Three of these nozzles were built around a plug since it provides space for storage.

The 12 chute nozzle was one which, in concept, would not be retracted. It did not divide the jet into as many segments as the others and had long chutes with gradual turning so that external air could reach the plug surface between segments of the primary jet. This nozzle was tested for performance at both take-off and supersonic cruise conditions in a static test facility.(42) A thrust performance penalty of 1.5% was obtained for both conditions referenced to an unsuppressed plug nozzle. The supersonic cruise penalty is rather large to pay for the major portion of the flight in order to obtain noise suppression at take-off.

The 48 tube nozzle had 6 nozzle boxes of 8 tubes each which, in concept, could be folded and stored within the plug. The 32 spoke nozzle was a General Electric Co. design. It was flight tested in cooperation with General Electric and results were reported in Refs. 38 and 39. In concept, the spokes would fold and be stored on the plug surface.

A tube suppressor nozzle designed for use with an auxiliary inlet ejector nozzle is shown in the lower right of Fig. 3(d). This nozzle was patterned after a Boeing Co. design.(43,44) The tubes would be mounted on 4 hinged segments which would swing away from the primary jet after take-off. This nozzle is shown with an acoustic treated shroud that could be removed. There was a similar shroud that was tested on the 12 chute and 48 tube nozzles.

The acoustic treated shrouds were made with a perforated inner liner followed by a bulk absorber consisting of stainless steel wire mesh. Cavity depths ranged up to 1.17 in. for the shroud used with the 12 chute and 48 tube nozzles and 1.80 in. for the one shown on the 104 tube nozzle. The 12 chute and 48 tube nozzles were tested with an acoustically treated plug as well as with a hard wall plug. The acoustically treated plug was fabricated from perforated sheet metal and a bulk absorber similar to that used on the shrouds.

Exhaust Jet Noise Measurements

It has been the practice to evaluate noise suppression devices on the basis of static tests. However, when the maximum sideline noise is reached during take-off the flight speed of advanced supersonic cruise aircraft can be as high as Mach 0.35. At these flight speeds external air flowing over the nozzle may affect its noise and thrust performance. The F106 flyover noise program was initiated to study these flight velocity effects.

The F106 was found to be uniquely suited for flyover noise measurements. The external flow environment was typical of supersonic cruise aircraft and exhaust nozzle configurations could be easily changed. Effects of external flow on noise directivity can be readily measured in flight. This is difficult if not impossible to do in the acoustic environment of wind tunnels. Flyover noise tests have been made on several exhaust nozzles and results are presented in Refs. 36 to 41.

Flyover passes were made at an altitude of 300 ft. and Mach number 0.4 with the main engine (J75) at idle (Fig. 4). One J85 engine was windmilled and the other was operated at a range of power settings up to maximum afterburning. Data from a microphone 4 feet above a concrete strip was tape recorded. Background noise levels produced by the airplane have been sufficiently below that produced by the various exhaust nozzles that no appreciable interference has occurred.(36-39)

Flight velocity effects were studied by comparing the flyover noise data to static data. Static data were obtained with the airplane on a concrete taxi strip with microphones located on a 100 ft radius from the exhaust nozzle. Ground runs were limited to nonafterburning operation of the J85. Thrust performance was determined using the load cell thrust measuring system[5] statically as well as in flyover.

Results and Discussion

Nozzle Installation Effects

The major installation effect observed during the early flight tests with the supersonic cruise nozzles was a reduction in boattail drag. The drag was reduced at high subsonic speeds and the drag rise was delayed to a Mach number of about 0.98. These effects are the result of a favorable location of the boattail downstream of the wing and interaction of the wing flow field with the nacelle terminal shock which moves on to the boattail as Mach number is increased in the subsonic speed range. This effect is further explained in References 20 to 23 and 27.

Detailed discussions of installation effects on these nozzles are contained in References 25 through 31. However, a summary comparison for the various nozzles is made in Fig. 5 at a Mach number of 0.9 and nozzle pressure ratio of 3.9. The variable flap ejector had the largest increase in installed performance due to a large reduction in boattail drag. The auxiliary inlet ejector also had a reduction in boattail drag but losses in admitting air through the auxiliary inlets resulted in little net installation benefit. The terminal shock interacted with the flow over the plug and wedge to produce higher pressures and thus raise installed performance for these nozzles by about 2%.

The variable flap ejector nozzle and the auxiliary inlet ejector were tested on the 22% F106 model.[25] Good agreement with flight data was obtained over most of the Mach number range for the variable flap ejector (Fig. 6). Disagreement occurred at Mach numbers near one, however, because of delay in passage of the terminal shock over the boattail in the wind tunnel due to model blockage effects.

For the auxiliary inlet ejector, however, poor agreement between flight and model performance was obtained at all Mach numbers. Since the inlet doors of the nozzle must obtain air from the nacelle boundary layer, the performance of nozzles of this type may be Reynolds number sensitive. At a Mach number of 0.9 Reynolds number for the 22% scale model was 18×10^6 and in flight it was 60×10^6 based on characteristic lengths as defined in the symbols. Thus the poor agreement between the two sets of data for this nozzle may be the result of Reynolds number differences.

Reynolds Number Effects

Another category of nozzle that appears to be Reynolds number sensitive is the supersonic dash nozzle, because of their steep boattail angles and large projected boattail areas (Fig. 3(b)). Data obtained with a circular arc and 3 circular arc-conic nozzles over a wide range of Reynolds number in flight confirmed that they were Reynolds number sensitive.[34] Boattail drag decreased with increasing Reynolds number over the range tested. This was caused by a decrease in the amount of separation on the boattail surface.

In subsequent tests the range of Reynolds number was extended to lower values by using data from the 5 and 22% models in addition to the flight data.[35] The trend observed in flight did not extend to the low Reynolds numbers of the wind tunnel models. Instead the drag peaked near the lowest flight Reynolds number and decreased to its lowest value for the lowest Reynolds number of the 5% scale model. These results are summarized schematically on Fig. 7. The solid lines shown are typical of the observed pressure distributions. The dashed lines represent the expected pressure distribution for inviscid flow.

At the highest Reynolds number the boundary layer over the nozzle was relatively thin and the observed pressure distribution exhibited the expected overexpansion at the shoulder and recompression to values above free stream static pressure. As the Reynolds number decreased the boundary layer thickened and this low energy flow had a tendency to separate. This reduced pressures in the recompression region on the boattail and the drag increased reaching a peak near the lowest flight Reynolds number. At the much lower Reynolds number of the 5% scale model the boundary layer became very thick in proportion to the nozzle diameter. This caused the overexpansion at the boattail shoulder to be reduced which reduced boattail drag.

The boattails reported in Refs. 34 and 35 had circular arc or combinations of circular arc and conic sections with primary emphasis on minimizing separation. The contoured nozzle of Fig. 3(c) might be expected to provide a different type of pressure distribution than the other nozzles.

Data have recently been obtained with the contoured nozzle and a comparison of its drag is made on Fig. 8 with drag from two boattail nozzles with circular arc and circular arc-conic cross sections (Fig. 3(b)). Reynolds number is based on a characteristic length of 5.18 meters (17 ft) which takes into consideration the wind chord (approximately 7.32 meters (24 ft)) and the nacelle length (approximately 3.96 meters (13 ft)) as in Ref. 34 and was appropriately scaled for the wind tunnel models. Drag of the contoured nozzle was as low as that of the longer circular arc nozzle and the same trends with Reynolds number were obtained. Boattail drag for both nozzles was relatively insensitive to Reynolds number over the flight range. However, boattail drag was negative (thrust) at the very low Reynolds number of the 5% scale model. The circular arc-conic nozzle which was similar in length to the contoured nozzle had considerably higher drag at the lowest flight Reynolds number. Increasing Reynolds number to the highest flight value decreased its drag to the same value as the other nozzles. At the lower Reynolds numbers of the 22% and 5% scale models, drag decreased but remained higher than for the other nozzles.

Pressure distributions for all three nozzles are shown on fig. 9 at the highest flight Reynolds

number. Data are shown along the bottom row of static pressure orifices, and are presented relative to the percentage of boattail area. The circular arc-conic nozzle had the largest overexpansion followed by recompression to a high value and some separation indicated by a flattening of the curve at about 80% of the boattail area. The circular arc nozzle had less overexpansion followed by a delayed recompression to a high value and very little or no separation. The contoured nozzle had the low overexpansion of the circular arc followed by a more rapid recompression and then separation over half the boattail area. These pressure distributions produced about the same boattail drag on all three nozzles.

Data at the lowest Reynolds number obtained in flight (Fig. 10) showed little change in pressure distribution for the contoured nozzle from that at the highest Reynolds number. The circular arc-conic nozzle had a less rapid recompression and more separation than previously. This accounts for its higher drag. The pressure distribution for the circular arc nozzle was little changed.

As Reynolds number was lowered further by going to the 5% scale model (Fig. 11), overexpansion at the shoulder was noticeably less for all nozzles. Also recompression was accomplished more rapidly and pressures on the aft portion were generally higher. The net result was the negative boattail drag shown on Fig. 8.

Even though the contoured nozzle always had separated flow over about half its projected area, it achieved a boattail drag as low as the circular arc nozzle. In making this comparison, it should be pointed out that the contoured nozzle was shorter and therefore potentially lighter. The contoured nozzle achieved low drag because of low overexpansion followed by a rapid recompression, in spite of a large amount of separation.

It was not always clear whether the flow over the nozzle boattails was separated or attached from pressure data alone. In order to clarify this, tufts mounted on the nozzle and photographed by a camera in the tail were very useful. Tuft photographs in Refs. 34 and 35 confirmed that for circular arc-conic and circular arc nozzles there was less tendency for flow to separate as Reynolds number increased in the flight range. The amount of separation also varied between nozzles.

Photographs of tufts on the contoured nozzle are shown in Fig. 12 at the lowest and highest values of flight Reynolds number. The dashed line represents the 50% boattail area location. The tufts show flow separation over the rear half of the boattail area in both cases. This might be expected based on the small change in boattail drag over this Reynolds number range (Fig. 8) and the flat pressure distribution curves of Figs. 9 and 10.

For nozzles which are sensitive to Reynolds number the difficulty of predicting full scale nozzle performance from wind tunnel model data is obvious. Pressure distributions obtained from subscale models can be considerably different from flight values because of boundary layer effects associated with low Reynolds number. To get reasonably accurate boattail drags, it appears to be necessary to have boattail shapes with very little separation or a relatively stable separated region such as obtained on the contoured nozzle. It also appears necessary to test at a minimum Reynolds number corresponding to about 30 million in the current case.

Flight Velocity Effects on Jet Noise Suppression

Flight velocity effects on noise and thrust performance of unsuppressed supersonic cruise type nozzles and several noise suppression nozzles have been previously reported in Refs. 36-41. A summary comparison of their performance is given in Fig. 13. In order to make the noise comparison, static noise data taken at 100 ft radius were adjusted to the 300 ft sideline condition of flyover. This was done using a computer program (Refs. 36 and 37) which accounted for the differences in distance, atmospheric attenuation, and ground effects. These data are all for a relative jet velocity (ideal jet velocity minus aircraft flight velocity) of 1760 ft/sec.

The peak noise levels during flyover were generally higher than predicted from static data by as much as 3.5 PNdB. However, the auxiliary inlet ejector and the 48 tube suppressor nozzle with shroud had lower flyover noise. The auxiliary inlet ejector nozzle was the noisiest under static conditions but had a large reduction in flyover noise.

With the auxiliary inlet ejector nozzle, extra air was admitted through inlet doors at low nozzle pressure ratio. Differences in the amount of this air entering the nozzle between static and flyover conditions may have accounted for its lower flyover noise.[36] There was also a change in the directivity of the noise pattern with this nozzle in flyover. The peak noise in flyover occurred at 40° from the jet centerline compared to 50° for static conditions.[36] This contributed to the lower peak noise in flyover because of the greater slant distance between the microphone and the source.

For the wedge nozzle, noise data were taken with the wedge in a vertical position for static data and horizontal for flyover data. This provided a similar orientation between the unsymmetrical wedge nozzle and the microphone during static and flyover testing.

Thrust performance for the unsuppressed nozzles was generally as high in flight as at static conditions. Thrust performance of the VFE nozzle was low both statically and in flyover because it was being operated in an overexpanded condition. Static thrust levels for the noise suppression nozzles were significantly below those of the unsuppressed nozzles. Also all the noise suppression nozzles suffered large additional thrust losses in flight except for the 12 chute nozzle. The largest single reason for the additional thrust loss in flyover was low pressure in base regions between tubes and on spokes.

The flight velocity effects on both noise suppression and thrust depend on the nozzle type. Flight velocity effects in most cases make the peak noise level higher and thrust lower.

Nozzle pressure ratio has an effect on gross thrust coefficient as shown on Fig. 14 for the 104

tube nozzle. The thrust decrement experienced in flyover becomes larger as the pressure ratio is decreased. This was typical of the performance observed with the other suppressor nozzles that were tested. Statically addition of the shroud provided about 2% higher thrust. In flyover no thrust increase was obtained when the shroud was installed.

The acoustic data from the flyover tests were scaled up to full size engines using the Strouhal number relationship and then adjusted to a sideline distance of 2128 ft for an altitude of 1000 ft. Jet noise suppression was obtained by referencing these noise levels to those from the plug nozzle scaled in a like manner. The effect on suppression of scaling and of increasing the distance between the noise source and the observer are shown in Fig. 15 for the 104 tube suppressor nozzle with acoustic shroud. The higher, more annoying frequencies were more dominant for the suppressor nozzle than for the plug nozzle. Scaling the spectrum to a larger nozzle lowered the frequencies into a less annoying range and increased the suppression 2 PNdB. Because the higher frequencies are more attenuated by the atmosphere a further suppression of 3 PNdB is obtained as the plug and suppressor noise are adjusted for distance. Also shown is the effect of time duration on suppression. Noise from this suppressor nozzle had a somewhat shorter time duration reducing the annoyance by 1 EPNdB relative to the reference plug nozzle. The magnitude and even the direction of these adjustments to full size and increased distance vary considerably depending on the nozzle under consideration.

Suppressor nozzle effectiveness in terms of effective perceived noise suppression versus percent thrust loss is presented in Fig. 16 for a full size aircraft. The 104 tube nozzle with acoustic shroud was the most effective (14.5 EPNdB for 14.3% thrust loss). The plain 104 tube nozzle had 12.5 EPNdB suppression and the shroud accounted for the remaining 2. The 12 chute nozzle also gave 1 EPNdB for 1% thrust loss but its maximum suppression was only 5 EPNdB. The shroud used with the 12 chute and 48 tube nozzles gave more suppression than obtained with the 104 tube shroud, but at considerable loss in thrust. The acoustic treated plug was found from comparisons not shown on the figure to give very little noise suppression. The J85 engine operates at jet exit velocities appropriate for turbofan engines. External flow effects may be different at the higher velocities and pressure ratios appropriate for turbojet engines.

Inlet Programs

For the flight program thus far discussed simple pitot inlets on the research nacelles have been adequate. Flight studies are now in progress with other inlet types which are appropriate for supersonic cruise and supersonic dash aircraft (Fig. 17).

Installation effects on inlets installed in an airframe flow field are being studied. The effects of inlet flow field on nozzle performance are being evaluated for some of the nozzles previously tested. Versions of these inlets will have throat Mach numbers increased to choking to study performance of inlets designed to suppress compressor noise.

There are two versions of the spike inlet. Other inlet types to be studied are a vertical wedge and a horizontal wedge.

The dynamic character of flow around the forebody of a fighter aircraft can be important to stable inlet-engine operation. Obtaining such data in the wind tunnel at angle of attack appropriate for current aircraft forces model blockage into a region where tunnel flow conditions can become questionable. A forebody model will be mounted on a boom from the nose of the F106 to obtain more nearly interference-free flow than available in wind tunnels. The flow field in the region of inlets will be surveyed in the transonic speed range with the model at angle of attack to 40° and yaw to 10°.

Concluding Remarks

A modified F106 aircraft has been used to study installation and flight velocity effects on exhaust nozzles. Wind tunnel data from an isolated nozzle test model and 5 and 22% scale F106 models were used for comparison. Static noise and thrust performance data obtained with the F106 for some of the nozzles were also used. From the results of over 240 flights which have been made since 1968 the following remarks can be made:

1. Installation effects: For nozzles mounted in aft underwing nacelles installation effects have been observed at high subsonic flight speeds. The effect is to decrease boattail drag and delay its drag rise Mach number to about 0.98. A nozzle having auxiliary inlets did not benefit as much as a simple variable flap ejector. Installed performance of plug and wedge nozzles was moderately higher than isolated at high subsonic flight speeds because of higher pressures on the plug and wedge surfaces.

2. Reynolds number effects: Boattail drag of nozzles for use on supersonic dash aircraft has been found to be sensitive to Reynolds number. In flight, drag was highest at the lowest Reynolds numbers obtained and decreased as Reynolds number was increased. At the lower Reynolds numbers of the scale models the boattail drag was lower. A contoured nozzle with a stable separated region and a full circular arc nozzle with little separation had similar drag levels and showed little drag variation over the flight Reynolds number range. A circular arc-conic nozzle that exhibited a large variation in the extent of separation between high and low Reynolds number had a large variation in drag and a high value of drag at the lowest flight Reynolds number.

3. Flight velocity effects on jet noise suppression: Static and flyover noise measurements made with several nozzles showed that except for special cases noise levels at take-off flight velocity (Mach number 0.4) were higher than predicted from static data. Thrust performance at static conditions for noise suppression nozzles was generally lower than for unsuppressed nozzles and was further degraded in flyover. Noise suppression effectiveness in terms of effective perceived noise level at a sideline distance of 2128 ft for engines scaled to full size but at 1760 ft per second relative jet velocity (typical of turbofan engines) reached levels of 14.5 EPNdB for 14.3% loss in thrust. Higher relative jet velocity operation would probably show greater suppression.

Symbols

A_{max} cross sectional area of cylindrical nacelle section (3166.9 cm^2 (490.9 $in.^2$))

C_D boattail drag coefficient, D/q_0A_{max}

C_p pressure coefficient, $(p - p_0)/q_0$

D diameter of cylindrical nacelle section, 63.5 cm (25 in.)

EPNL effective perceived noise level, EPNdB

$\frac{F - D}{F_{ip}}$ nozzle gross thrust coefficient

M_0 free stream Mach number

PNL perceived noise level, PNdB

P_8/P_0 nozzle pressure ratio

Re Reynolds number based on a characteristic length of 5.18 m (17 ft) for flight and appropriately scaled values for the wind tunnel models

X axial distance along boattail

Y radial dimension from nozzle centerline to outer surface

Nozzle abbreviations:

AIE auxiliary inlet ejector

VFE variable flap ejector

References

1. Crabs, C. C., Boyer, E. O., and Mikkelson, D. C., "Engineering Aspects and First Flight Results of the NASA F-106 Transonic Propulsion Research Aircraft," TM X-52559, 1969, NASA Cleveland, Ohio.

2. Wilcox, F. A., Samanich, N. E., and Blaha, B. J., "Flight and Wind Tunnel Investigation of Installation Effects on Supersonic Cruise Exhaust Nozzles at Transonic Speeds," Paper 69-427, Apr. 1969, AIAA, New York, N.Y.

3. Crabs, C. C., Mikkelson, D. C., and Boyer, E. O., "An Inflight Investigation of Airframe Effects on Propulsion System Performance at Transonic Speeds," Society of Experimental Test Pilots, Technical Review, Vol. 9, No. 4, 1969, pp. 51-66.

4. Groth, H. W., Samanich, N. E., and Blumenthal, P. Z., "Inflight Thrust Measuring System for Underwing Nacelles Installed on a Modified F-106 Aircraft," TM X-2356, 1971, NASA Cleveland, Ohio.

5. Groth, H. W., "Nozzle Performance Measurement on Underwing Nacelles of an F-106 Utilizing Calibrated Engines and Load Cells;" Paper 71-681, June 1971, AIAA, New York, N.Y.

6. Bresnahan, D. I., and Johns, A. L., "Cold Flow Investigation of a Low Angle Turbojet Plug Nozzle With Fixed Throat and Translating Shroud at Mach Numbers from 0 to 2.0," TM X-1619, 1968, NASA, Cleveland, Ohio.

7. Steffen, F. W., and Jones, J. R., "Performance of a Wind Tunnel Model of an Aerodynamically Positioned Variable Flap Ejector at Mach Numbers from 0 to 2.0," TM X-1639, 1968, NASA. Cleveland, Ohio.

8. Bresnahan, D. L., "Experimental Investigation of a 10° Conical Turbojet Plug Nozzle with Iris Primary and Translating Shroud at Mach Numbers from 0 to 2.0," TM X-1709, 1968, NASA, Cleveland, Ohio.

9. Blaha, B. J., and Bresnahan, D. L., "Wind Tunnel Installation Effects on Isolated Afterbodies at Mach Numbers from 0.56 to 1.5," TM X-52581, 1969, NASA, Cleveland, Ohio.

10. Bresnahan, D. L., "Experimental Investigation of a 10° Conical Turbojet Plug Nozzle with Translating Primary and Secondary Shrouds at Mach Numbers from 0 to 2.0," TM X-1777, 1969, NASA, Cleveland, Ohio.

11. Harrington, D. E., "Jet Effects on Boattail Pressure Drag of Isolated Ejector Nozzles at Mach Numbers from 0.60 to 1.47," TM X-1785, 1969, NASA, Cleveland, Ohio.

12. Bresnahan, D. L., "Performance of an Aerodynamically Positioned Auxiliary Inlet Ejector Nozzle at Mach Numbers from 0 to 2.0," TM X-2023, 1970, NASA, Cleveland, Ohio.

13. Johns, A. L., and Steffen, F. W., "Performance of an Auxiliary Inlet Ejector Nozzle with Fixed Doors and Single-Hinge Trailing-Edge Flap," TM X-2027, 1970, NASA, Cleveland, Ohio.

14. Johns, A. L., and Steffen, F. W., "Performance of an Auxiliary Inlet Ejector Nozzle with Fixed Inlet Doors and Triple-Hinge Trailing-Edge Flap," TM X-2034, 1970, NASA, Cleveland, Ohio.

15. Steffen, F. W., and Johns, A. L., "Performance of a Fixed Geometry Wind Tunnel Model of an Auxiliary Inlet Ejector with a Clamshell Flow Diverter from Mach 0 to 1.2," TM X-2037, 1970, NASA, Cleveland, Ohio.

16. Harrington, D. E., "Performance of Convergent and Plug Nozzles at Mach Numbers from 0 to 1.97," TM X-2112, 1970, NASA, Cleveland, Ohio.

17. Harrington, D. E., "Performance of a 10° Conical Plug Nozzle with Various Primary Flap and Nacelle Configurations at Mach Numbers from 0 to 1.97," TM X-2086, 1970, NASA, Cleveland, Ohio.

18. Johns, A. L., "Performance of an Auxiliary Inlet Ejector Nozzle with Floating Inlet Doors and Floating Single-Hinge Trailing-Edge Flaps," TM X-2173, 1971, NASA, Cleveland, Ohio.

19. Blaha, B. J., and Johns, A. L., "Effect of Exit Area Variation on the Performance of an Auxiliary Inlet Ejector Nozzle at Mach Numbers

from 0 to 1.27," TM X-2182, 1971, NASA, Cleveland, Ohio.

20. Blaha, B. J., and Mikkelson, D. C., "Wind Tunnel Investigation of Airframe Installation Effects on Underwing Engine Nacelles at Mach Numbers from 0.56 to 1.46," TM X-1683, 1968, NASA, Cleveland, Ohio.

21. Blaha, B. J., Mikkelson, D. C., and Harrington, D. E., "Wind Tunnel Investigation of Installation Effects on Underwing Supersonic Cruise Exhaust Nozzles at Transonic Speeds," TM X-52604, 1969, NASA, Cleveland, Ohio.

22. Blaha, B. J., "Effect of Underwing Engine Nacelle Shape and Location on Boattail Drag and Wing Pressures at Mach Numbers from 0.56 to 1.46," TM X-1979, 1970, NASA, Cleveland, Ohio.

23. Mikkelson, D. C., and Blaha, B. J., "Flight and Wind Tunnel Investigation of Installation Effects on Underwing Supersonic Cruise Exhaust Nozzles at Transonic Speeds," TM X-52827, 1970, NASA, Cleveland, Ohio.

24. Blaha, B. J., "Wind Tunnel Investigation of the Flow Field Under a 60-Degree Swept Wing at Mach Numbers from 0.6 to 2.0," TM X-52585, 1969, NASA, Cleveland, Ohio.

25. Steffen, F. W., Satmary, E. A., Vanco, M. R., and Nosek, S. M., "A Turobjet Simulator for Mach Numbers up to 2.0," TM X-67973, 1971, NASA, C leveland, Ohio.

26. Samanich, N. E., and Burley, R. R., "Flight Performance of Auxiliary Inlet Ejector and Plug Nozzle at Transonic Speeds," Paper 70-701, Apr. 1970, AIAA, New York, N.Y.

27. Mikkelson, D. C., and Head, V. L., "Flight Investigation of Airframe Installation Effects on a Variable Flap Ejector Nozzle of an Underwing Engine Nacelle at Mach Numbers from 0.5 to 1.3," TM X-2010, 1970, NASA, Cleveland, Ohio.

28. Samanich, N. E., and Chamberlin, R., "Flight Investigation of Installation Effects on a Plug Nozzle Installed on an Underwing Nacelle," TM X-2295, 1971, NASA, Cleveland, Ohio.

29. Burley, R. R., "Flight Investigation of Airframe Installation Effects on an Auxiliary Inlet Ejector Nozzle on an Underwing Engine Nacelle," TM X-2396, 1971, NASA, Cleveland, Ohio.

30. Head, V. L., "Flight Investigation of an Underwing Nacelle Installation of Three Variable-Flap Ejector Nozzles," TM X-2478, 1972, NASA, Cleveland, Ohio.

31. Head, V. L., "Flight Investigation of an Underwing Nacelle Installation of an Auxiliary-Inlet Ejector Nozzle with a Clamshell Flow Diverter from Mach 0.6 to 1.3," TM X-2655, 1972, NASA, Cleveland, Ohio.

32. Samanich, N. E., "Flight Investigation of an Air-Cooled Plug Nozzle with an Afterburning Turbojet," TM X-2607, 1972, NASA, Cleveland, Ohio.

33. Johns, A. L., and Jeracki, R. J., "Preliminary Investigation of Performance of a Wedge Nozzle Applicable to a Supersonic-Cruise Aircraft," TM X-2169, 1971, NASA, Cleveland, Ohio.

34. Chamberlin, R., "Flight Investigation of 24° Boattail Nozzle Drag at Varying Subsonic Flight Conditions," TM X-2626, 1972, NASA, Cleveland, Ohio.

35. Chamberlin, R., and Blaha, B. J., "Flight and Wind Tunnel Investigation of the Effects of Reynolds Number on Installed Boattail Drag at Subsonic Speeds," Paper 73-139, Jan. 1973, AIAA, New York, N.Y.

36. Burley, R. R., and Karabinus, R. J., "Flyover and Static Tests to Investigate External Flow Effects on Jet Noise for Non-Suppressor and Suppressor Exhaust Nozzles," Paper 73-190, Jan, 1973, AIAA, New York, N.Y.

37. Burley, R. R., Karabinus, R. J., and Freedman, R. J., "Flight Investigation of Acoustic and Thrust Characteristics of Several Exhaust Nozzles Installed on Underwing Nacelles on an F-106 Aircraft," TM X-2854, 1973, NASA, Cleveland, Ohio.

38. Brausch, J. F, "Flight Velocity Influence on Jet Noise of Conical Ejector, Annular Plug and Segmented Suppressor Nozzles," NASA CR-120961, Aug. 1972, General Electric Co., Evendale, Ohio.

39. Chamberlin, R., "Flyover and Static Tests to Investigate Flight Velocity Effects on Jet Noise of Suppressed and Unsuppressed Plug Nozzle Configurations," TM X-2856, 1973, NASA, Cleveland, Ohio.

40. Burley, R. R., and Johns, A. L., "Flight Velocity Effects on the Jet Noise of Several Variations of a 12-Chute Suppressor Installed on a Plug Nozzle," TM X-2918, 1973, NASA, Cleveland, Ohio.

41. Burley, R. R., and Head, V. L., "Flight Velocity Effects on the Jet Noise of Several Variations of a 48-Tube Suppressor Installed on a Plug Nozzle," TM X-2919, 1973, NASA, Cleveland, Ohio.

42. Bresnahan, D. L., "Internal Performance of a 10° Conical Plug Nozzle with a Multispoke Primary and Translating External Shroud," TM X-2573, 1972, NASA, Cleveland, Ohio.

43. Swann, W. C., and Simcox, C. D., "A Status Report on Jet Noise Suppression as Seen by an Aircraft Manufacturer," The First International Symposium on Air Breathing Engines, June 1972.

44. Anon., "SST Technology Follow-On Program - Phase 1, A Summary of the SST Noise Suppression Test Program," FAA-SS-72-41, Feb. 1972, Boeing Co., Seattle, Wash.

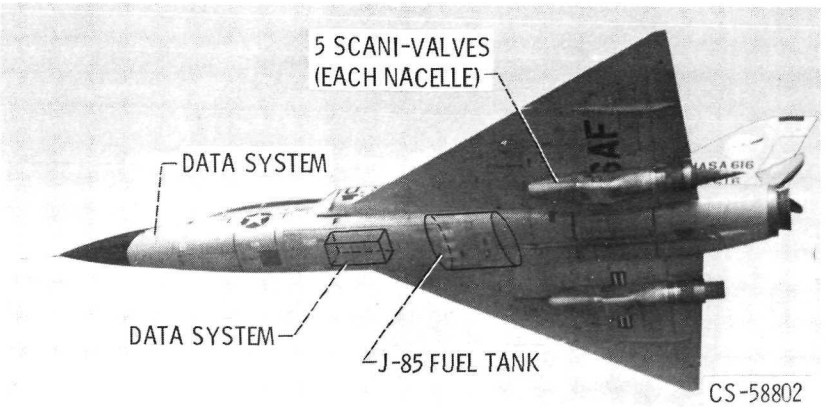

Figure 1. - Modifications to F106.

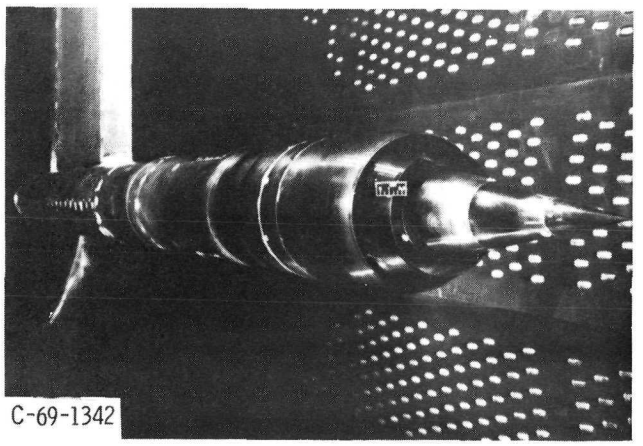

ISOLATED NOZZLE

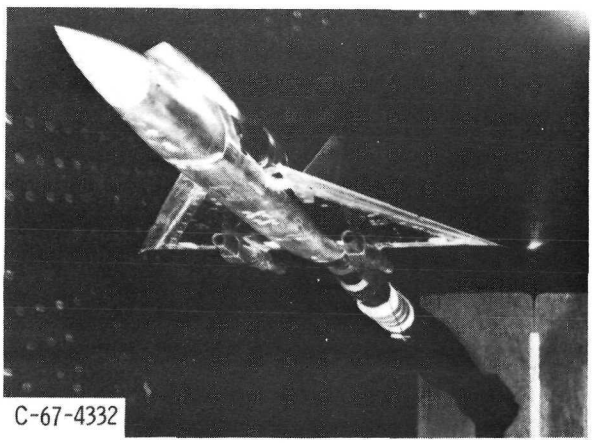

5% SCALE F106

22% SCALE F106

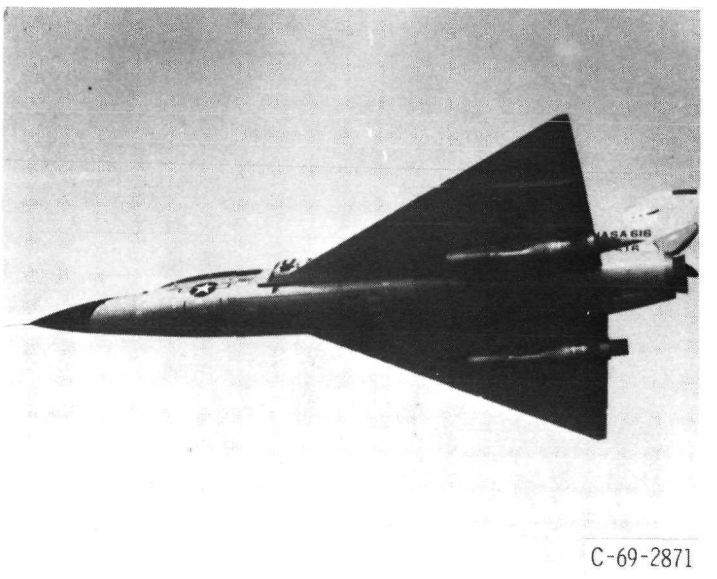

F106 FLIGHT

Figure 2. - Wind tunnel and flight test models.

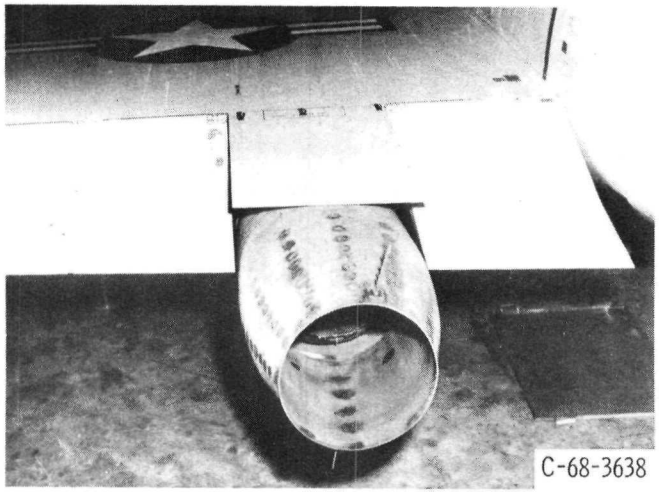

VARIABLE FLAP EJECTOR (VFE)

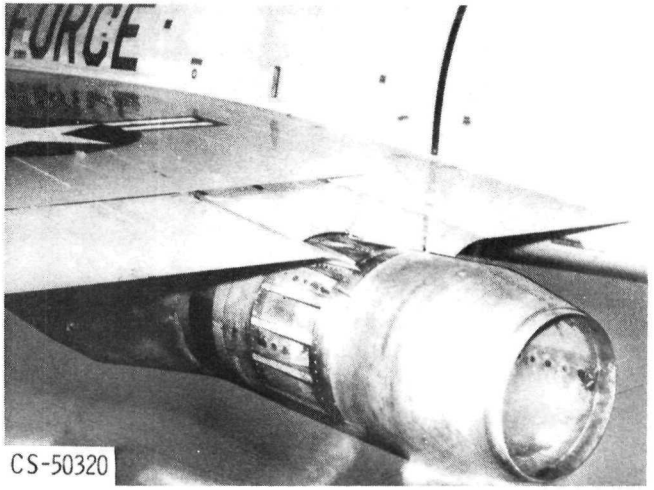

AUXILIARY INLET EJECTOR (AIE)

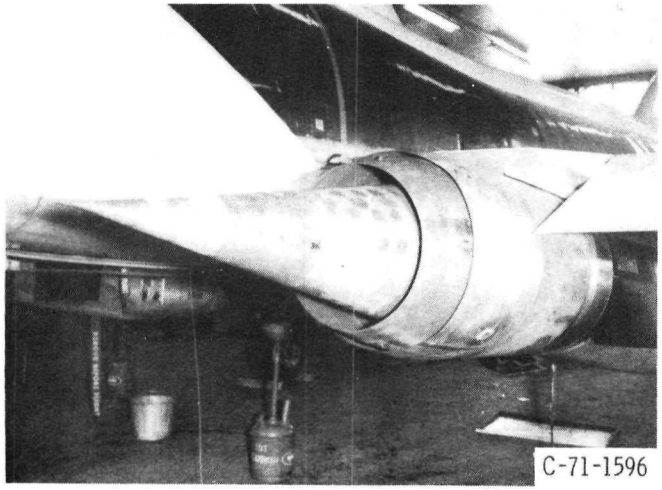

PLUG

WEDGE

(a) SUPERSONIC CRUISE NOZZLES.

Figure 3. - Exhaust nozzles.

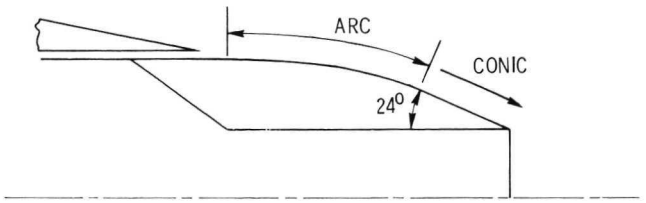

CIRCULAR ARC-CONIC

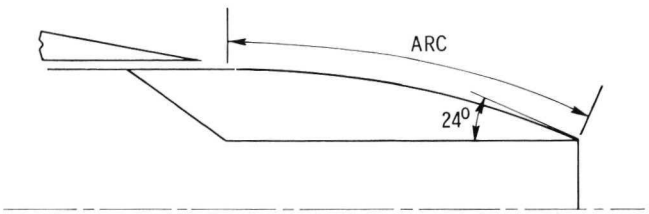

CIRCULAR ARC

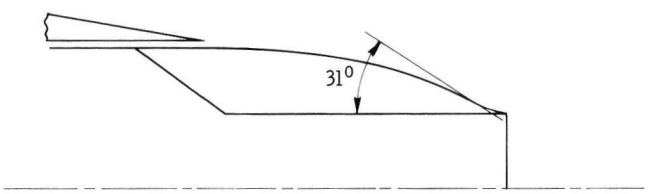

CONTOURED

(B) SUPERSONIC DASH NOZZLES.

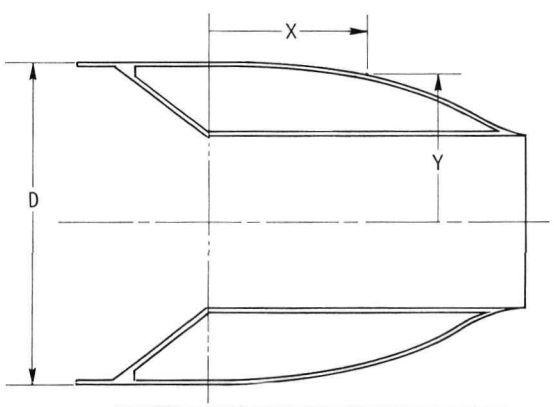

AXIAL DIMENSION, X/D	RADIAL DIMENSION, Y/D
0	0.5
.08	.499
.16	.497
.24	.494
.32	.487
.40	.475
.48	.461
.56	.439
.64	.409
.72	.372
.80	.328
.84	.304
.88	.288
.92	.276
.95	.272

(C) DIMENSIONS OF CONTOURED NOZZLE.

Figure 3. - Continued.

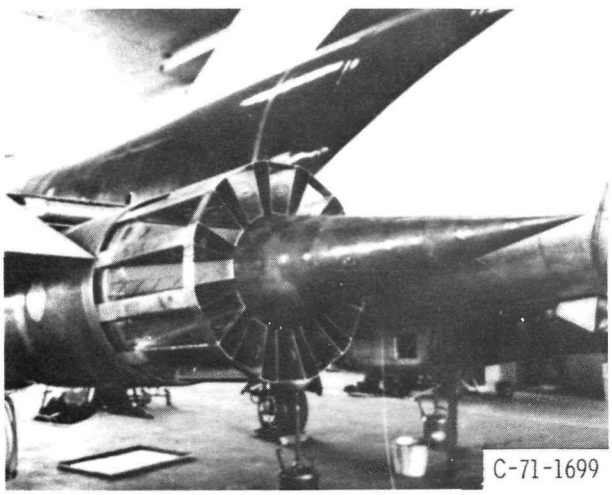

12 CHUTE

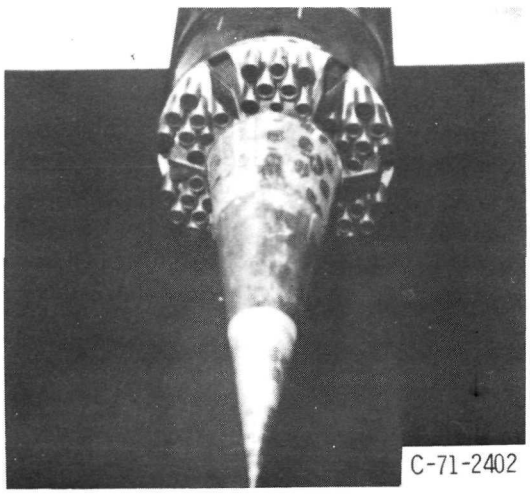

48 TUBE

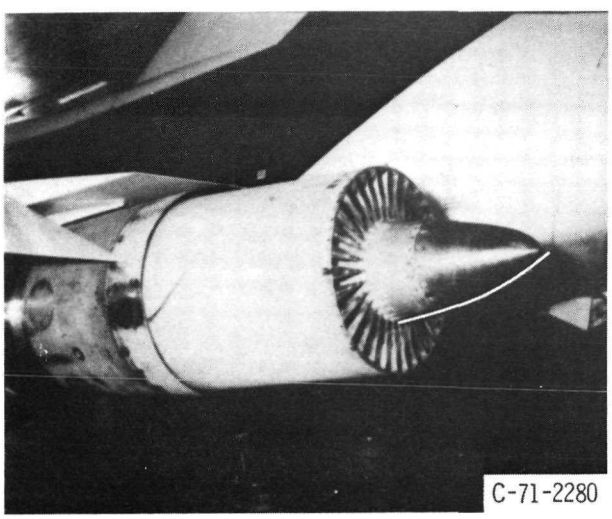

32 SPOKE

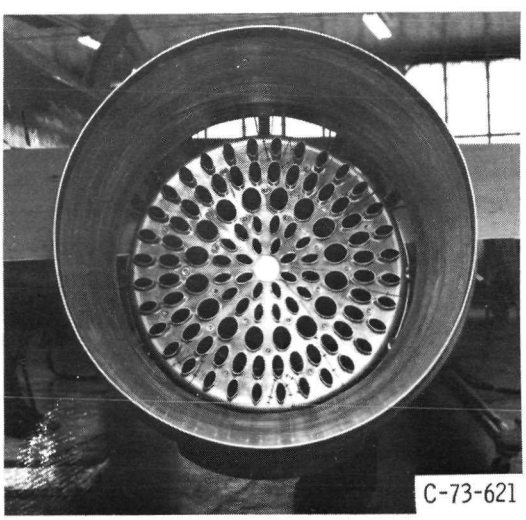

104 TUBE WITH ACOUSTIC SHROUD

(d) NOISE SUPPRESSION NOZZLES.

Figure 3. - Concluded.

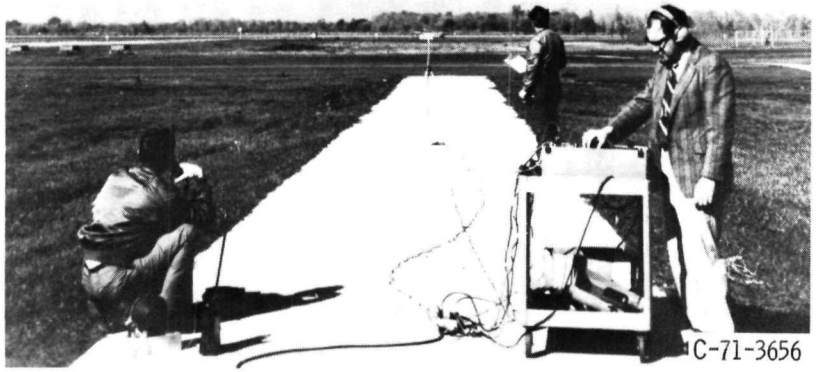

Figure 4. - Flyover noise tests.

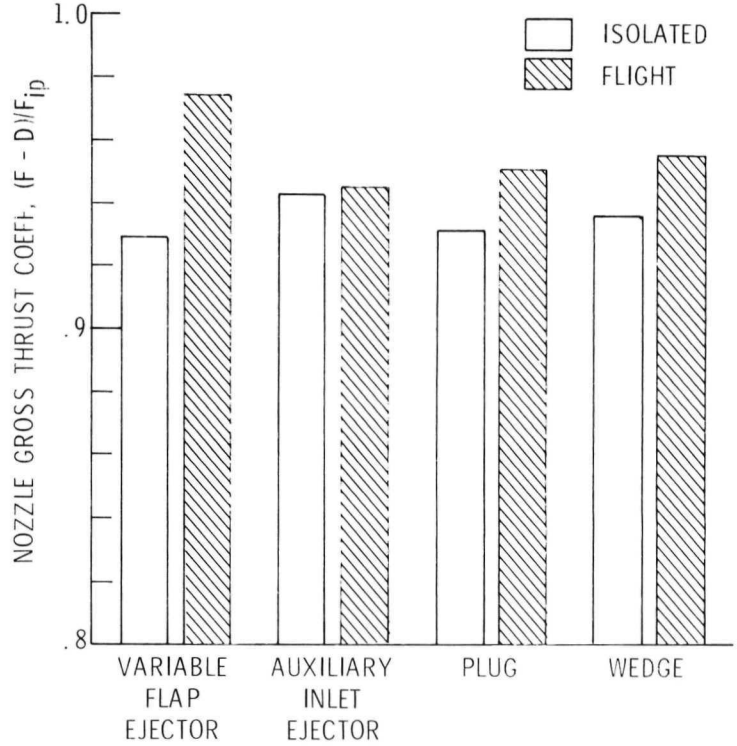

Figure 5. - Nozzle installation effects, $M_0 = 0.9$, $P_8/p_0 = 3.9$. Nominal corrected secondary flow 3% (4% for wedge).

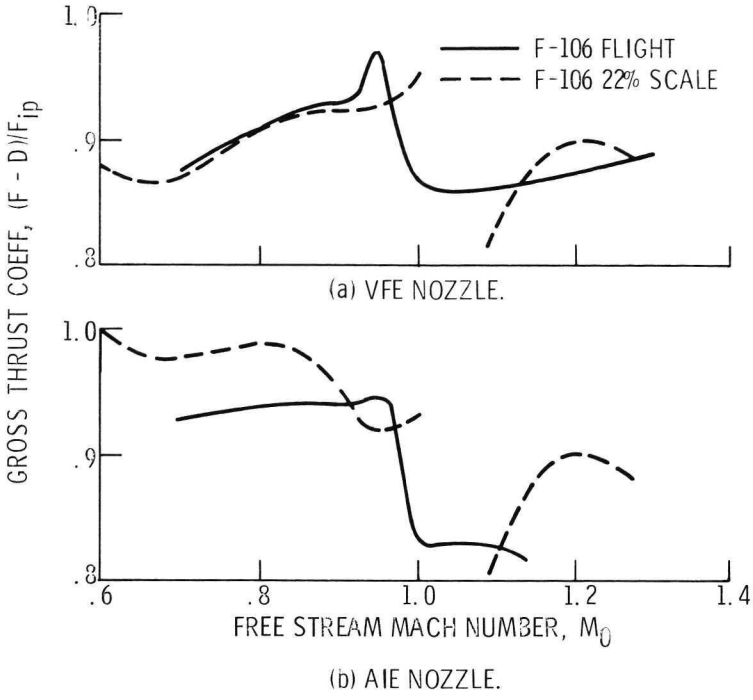

Figure 6. - Comparison of nozzle performance in flight and on 22% scale model.

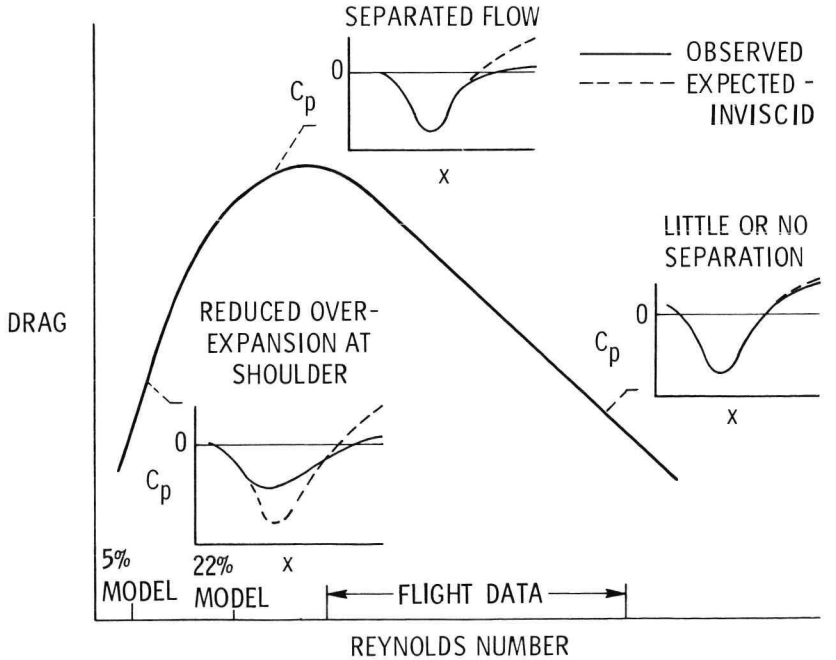

Figure 7. - Summary of Reynolds number effects.

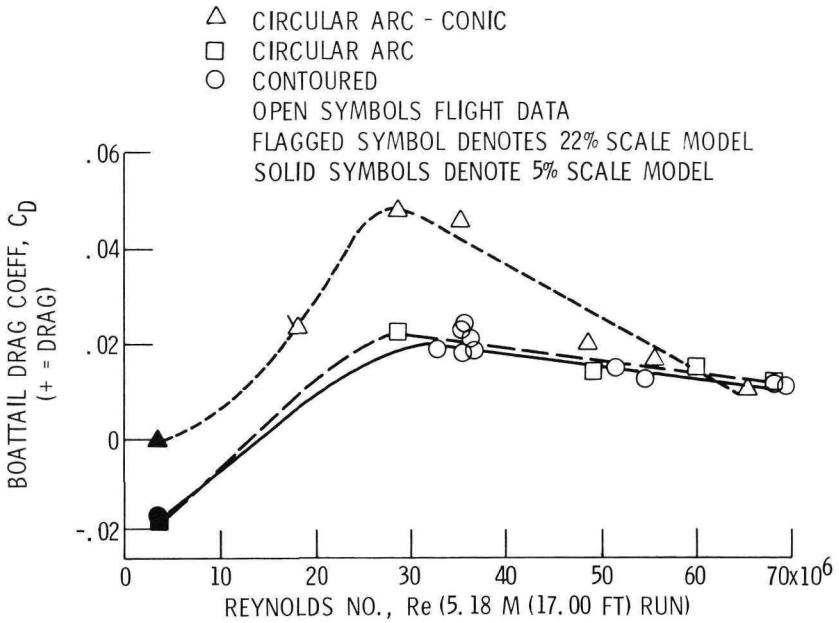

Figure 8. - Effect of Reynolds number on boattail drag for 3 supersonic dash nozzles. Mach 0.9.

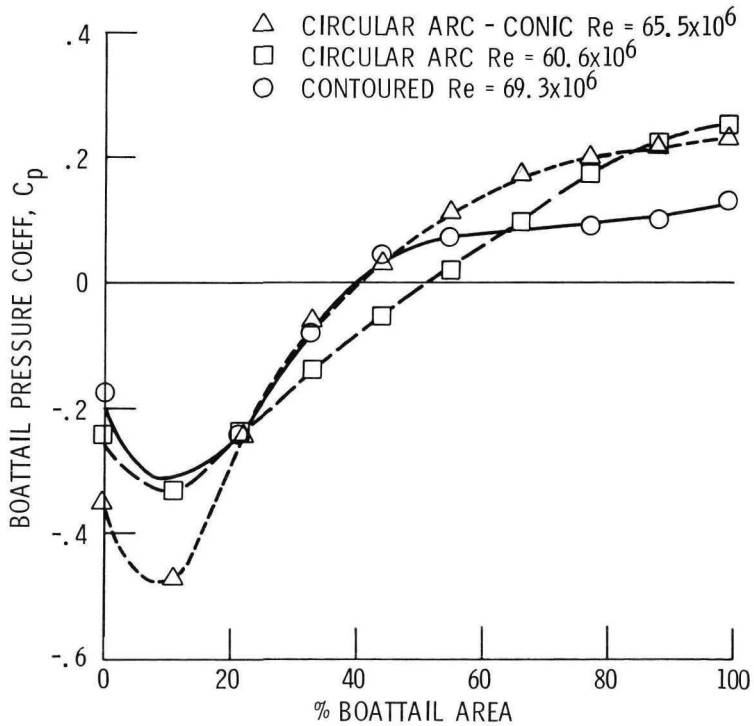

Figure 9. - Boattail pressure distribution at highest flight Reynolds number for 3 supersonic dash nozzles. Mach 0.9; 180^0 meridian angle.

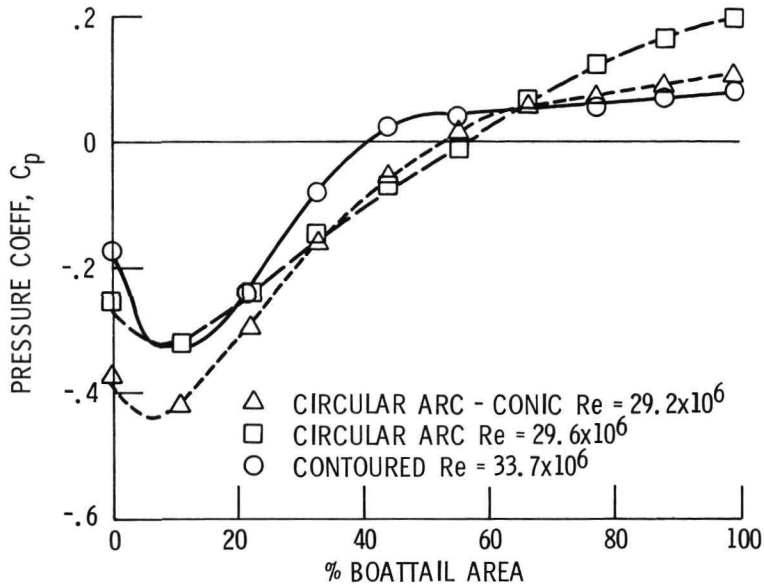

Figure 10. - Boattail pressure distribution at lowest flight Reynolds number for 3 supersonic dash nozzles. Mach 0.9; 180^0 meridian angle.

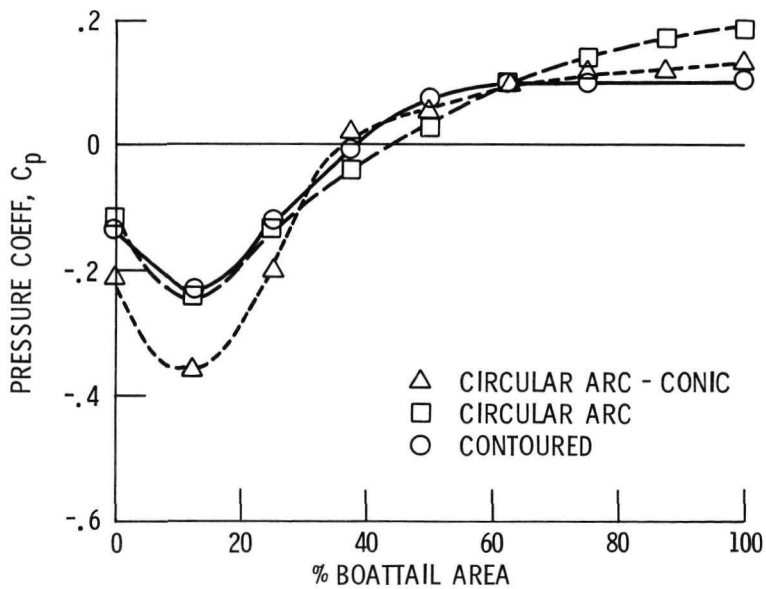

Figure 11. - Boattail pressure distribution from 5% scale F106 model for 3 supersonic dash nozzles. Mach 0.9; 180^0 meridian angle; Reynolds number = 3.5x10^6.

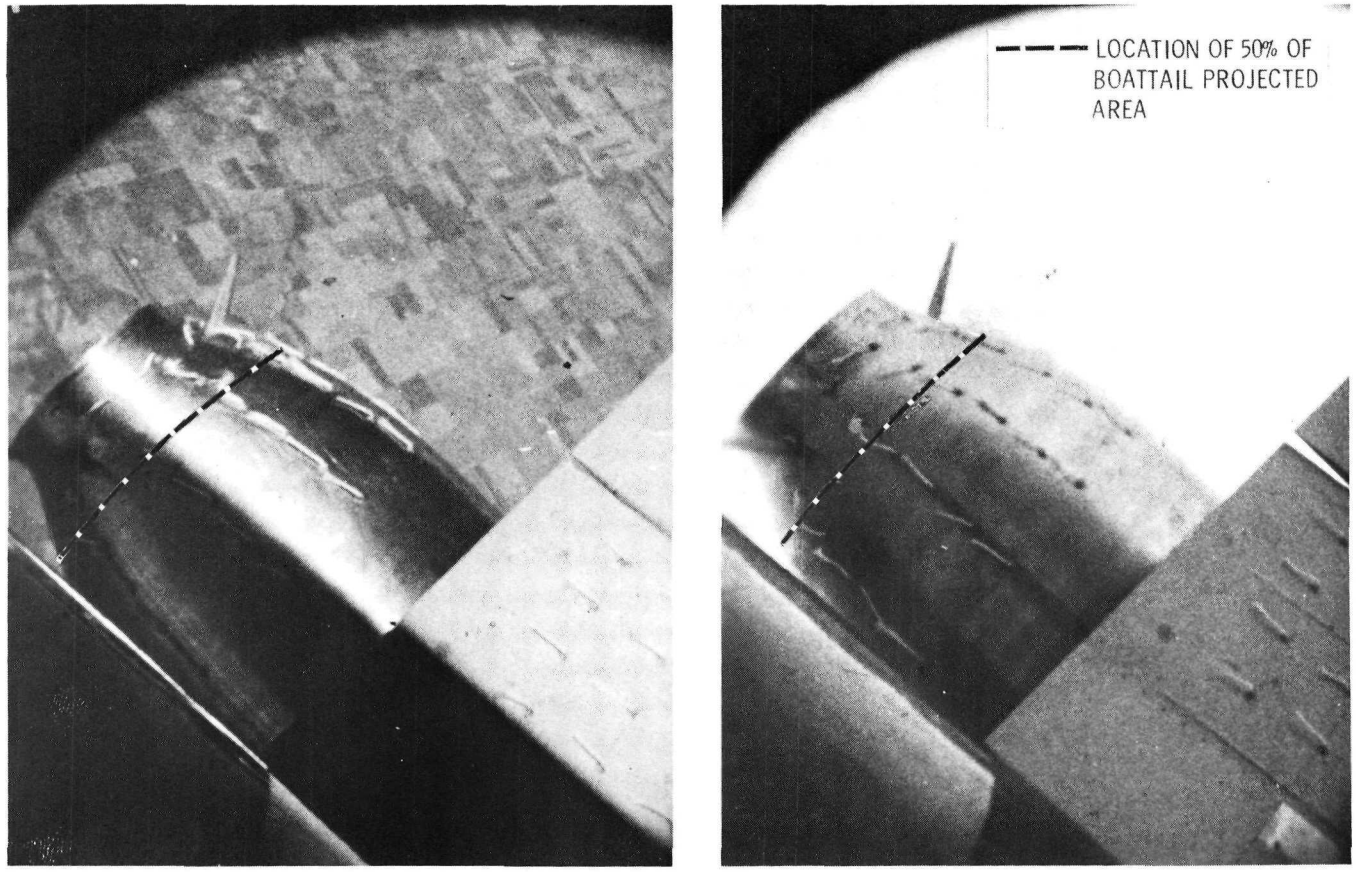

Re = 35.7×10^6 Re = 69.4×10^6

Figure 12. - Tuft photographs at high and low Reynolds No. with contoured nozzle; $M_0 = 0.9$; angle of attack, 4^0.

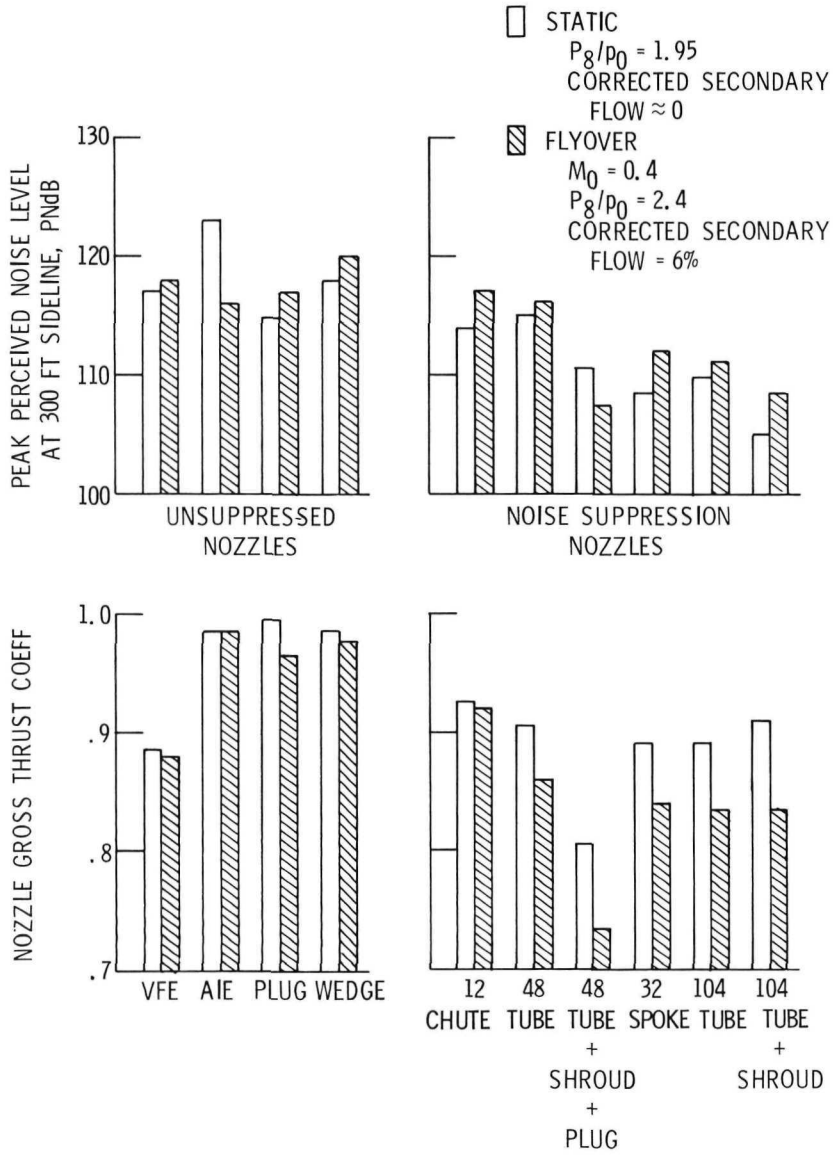

Figure 13. - Flight velocity effects on nozzle peak noise and thrust performance. Relative jet velocity, 1760 ft/sec.

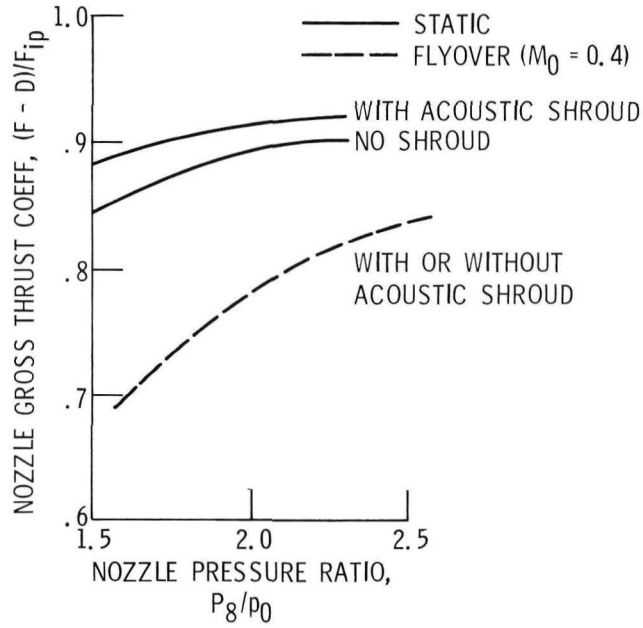

Figure 14. - Nozzle pressure ratio effect on thrust coefficient. 104 Tube nozzle with and without acoustic shroud.

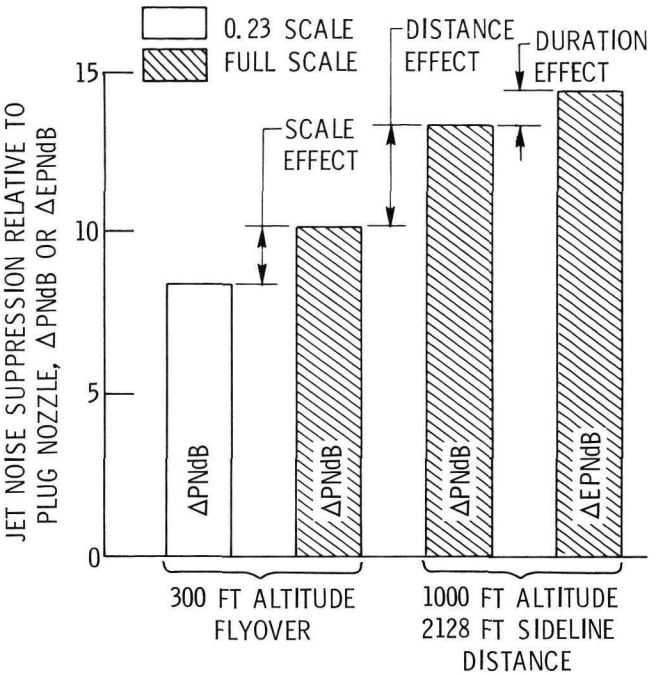

Figure 15. - Effect of scale, distance, and duration on noise suppression of 104 tube nozzle with acoustic shroud.

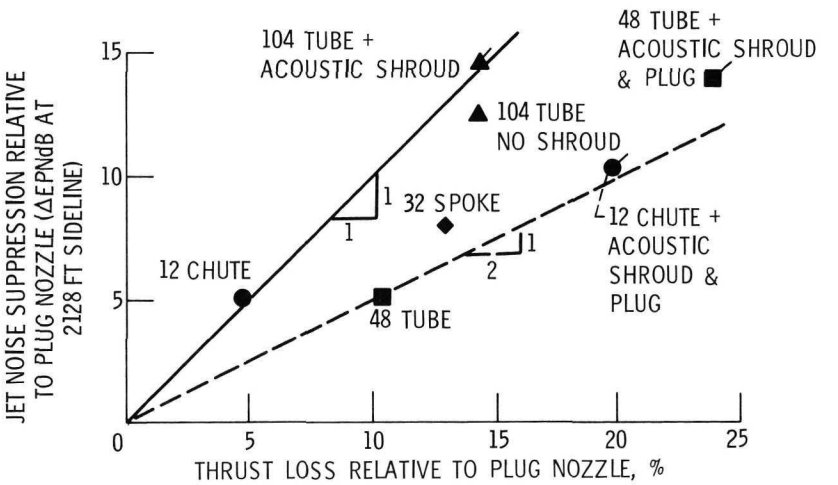

Figure 16. - Noise suppression nozzle effectiveness scaled to full size engine, 2128 ft sideline distance, altitude = 1000 ft, Mach no. = 0.4.

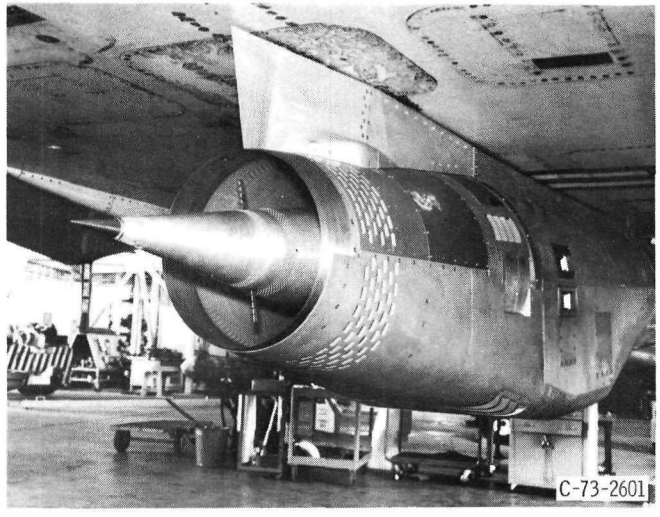

SPIKE INLET

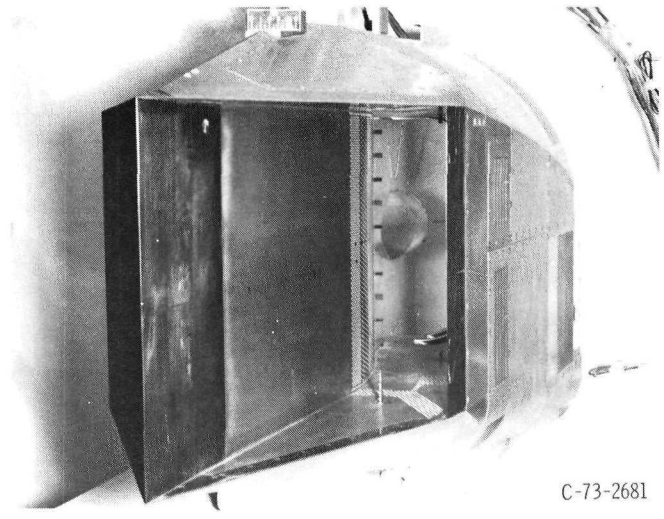

VERTICAL WEDGE INLET

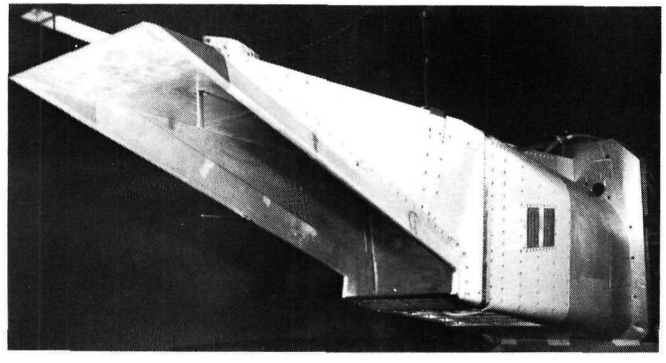

HORIZONTAL WEDGE INLET

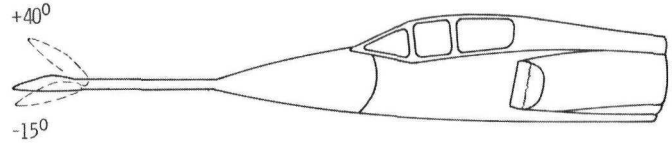

FOREBODY MODEL MOUNTED ON F106

NASA-Lewis

Figure 17. - Inlets and forebody model.